Int. J. Solids Structures, 1971, Vol. 7, pp. 1057 to 1073. Pergamon Press. Printed in Great Britain

ON AN ANALOGY BETWEEN PLANE STRAIN AND PLATE BENDING SOLUTIONS IN RIGID/PERFECT PLASTICITY THEORY

I. F. COLLINS

Department of Mathematics, University of Manchester Institute of Science and Technology

Abstract—This paper presents the theory underlying Johnson's recent analogy between upper bound solutions for rigid/perfectly-plastic materials in plane strain and in plate bending theory. This analogy is extended to lower bound and complete solutions. Many exact solutions in plane strain, such as the classical Prandtl punch solution, can be interpreted as exact solutions to plate bending problems. As an illustration of a slip-line field technique which can be taken over into plate theory, Bishop's method of completing slip-line solutions is used to complete a yield-line theory solution for a centrally-loaded simply-supported rectangular plate. Recent solutions to this and similar problems due to Sawczuk and Hodge are shown to be in error.

1. INTRODUCTION

IN A recent paper Johnson [1] has discussed an interesting analogy between the techniques for calculating upper bounds to rigid/plastic yield-point loads in plane strain and in thin plate bending theory. As is well known, overestimates of yield point loads can be obtained from any kinematically admissible deformation mode, by equating the rate of working of the applied loads to the rate of energy dissipation within the body. In plane strain situations this technique has been extensively developed with particular regard to problems of metal forming processes [2]; whilst in the theory of plates and reinforced concrete slabs it is one of the techniques of yield-line theory [3–6].

The essence of Johnson's analogy is the identification of the *velocity* in a typical plane strain upper bound mode with the *angular velocity* in the corresponding mode for an isotropic plate. The trajectories of maximum shear strain-rate or slip-lines in plane strain correspond to the principal curvature-rate trajectories or yield lines in the analogous plate problem. In [1] this analogy is applied to a number of standard plane strain solutions in order to derive upper bounds to the yield loads in the corresponding plate problems.

In the conventional approach to yield-line theory it seems usual to assume that one family of yield-lines consists of straight lines (cf. [3–6]). However, slip-line field solutions frequently contain regions in which both families of slip-lines are curved. Thus, Johnson's upper bound modes are intrinsically more general than those of conventional yield-line theory, and hence may be expected to frequently give rather better approximations to the actual loads.

The main purpose of the present paper is to develop this analogy a step further and show that there is a dual, though rather more restricted, correspondence between the statics of the two classes of problems. This extended analogy enables one to interpret *lower bound* solutions in plane strain as lower bound solutions in plate theory. Further, by combining the two analogies one can obtain a correspondence between *exact* solutions

in the two classes of problems. This quasi-static analogy stems from the fact that *in the absence of distributed loads* the equilibrium equations demand that the pattern of yield-lines must satisfy the Hencky–Prandtl property when the plastic stress state is at one or other of two of the corners of the Johansen square yield locus. The Hencky–Prandtl property is, of course, the characterizing property of slip-line fields [7, 8]. This seems first to have been noted by Schumann [9], though with reference to the corresponding points on the Tresca yield locus.

This static analogy is described in detail in Section 2, where it is made explicit by the introduction of a stress function ψ for the shear forces. This stress function plays the role of the hydrostatic pressure in the analogous plane strain theory. The theory underlying Johnson's kinematic analogy is given in Section 3 where in particular, the properties of the angular velocity hodograph diagram are derived. The classical Prandtl punch solution is discussed in Section 4 as an example of an exact plane strain solution which can be interpreted as an exact plate solution.

It is thought, however, that the main use of these analogies will be the application of the extensively developed techniques for constructing solutions in plane strain to plate problems whose plane strain analogue is not practically meaningful. Examples are the use of the hodograph diagram in formulating kinematic boundary conditions and the method of extending a slip-line solution into a postulated rigid region in order to show that the solution is "complete". In illustration the problem of a simply supported plate with a central point load is considered in Sections 5 and 6. Improved upper bound loads are obtained for a certain range of aspect ratios, whilst the yield-line theory solution is completed and shown to be exact provided the aspect ratio exceeds 3·10. Sawczuk and Hodge [10] have also recently discussed this problem and presented a solution which involves Hencky–Prandtl nets. However, as discussed in detail in Section 5, their solution is erroneous.

2. THE STATIC ANALOGY

The governing equations of rigid perfectly-plastic plate theory were first analysed by Hopkins [11] and Schumann [9]. Both these authors used the Tresca yield criterion and associated flow rule. However, these analyses are readily adapted to the square yield criterion and its associated flow rule and have been given by Massonnet [12] and Sawczuk and Hodge [10]. A general analysis applicable to any isotropic yield criterion and associated flow rule has been given by Hodge [13].

Referred to a Cartesian (x, y) co-ordinate system the equilibrium equations for a thin plate in bending are:

$$\frac{\partial M_x}{\partial x}+\frac{\partial M_{xy}}{\partial y}-Q_x=0 \tag{2.1}$$

$$\frac{\partial M_{xy}}{\partial x}+\frac{\partial M_y}{\partial y}-Q_y=0 \tag{2.2}$$

$$\frac{\partial Q_x}{\partial x}+\frac{\partial Q_y}{\partial y}=-q \tag{2.3}$$

where (M_x, M_y, M_{xy}) are the components of the moment tensor, (Q_x, Q_y) are the components of the shear force vector and $q(x, y)$ is the transverse loading distribution.

Alternatively, the equilibrium equations can be referred to the curvilinear principal stress trajectories (α- and β-curves):

$$\frac{\partial M_\alpha}{\partial s_\alpha}+\frac{M_\alpha-M_\beta}{\rho_\beta}-Q_\alpha=0 \tag{2.4}$$

$$\frac{\partial M_\beta}{\partial s_\beta}+\frac{M_\beta-M_\alpha}{\rho_\alpha}-Q_\beta=0 \tag{2.5}$$

$$\frac{\partial Q_\alpha}{\partial s_\alpha}+\frac{\partial Q_\beta}{\partial s_\beta}+\frac{Q_\alpha}{\rho_\beta}+\frac{Q_\beta}{\rho_\alpha}=-q \tag{2.6}$$

where M_α, M_β are the principal moments; Q_α, Q_β the corresponding shear force components; s_α, s_β the arc-lengths of the principal stress trajectories and ρ_α, ρ_β their radii of curvature defined by:

$$\frac{1}{\rho_\alpha}=-\frac{\partial\varphi}{\partial s_\alpha}, \qquad \frac{1}{\rho_\beta}=\frac{\partial\varphi}{\partial s_\beta} \tag{2.7}$$

φ being the anticlockwise rotation of the α-curve from the x-axis.

There are three basic types of plastic stress state associated with Johansen's square yield criterion, (assuming equal top and bottom reinforcement) [Fig. 1(a)] exemplified by the two singular points A, B and the side AB of the yield locus. These are described in detail in [10] and will only briefly be recapitulated here.

Regime A

This regime represents an isotropic stress state since $M_\alpha = M_\beta = M$ and can only occur in a *finite* region if $q = Q_\alpha = Q_\beta = 0$.

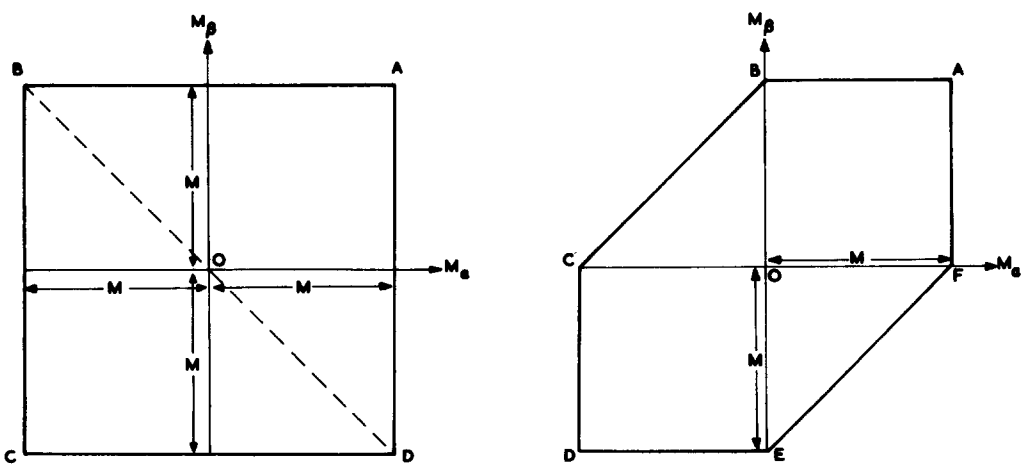

FIG. 1. Yield loci for isotropic plates: (a) Johansen's square locus for reinforced concrete slabs with equal top and bottom reinforcement; (b) Tresca's criterion.

Regime AB

From the normality property of the associated flow rule the principal component κ_α of the curvature-rate tensor $(\kappa_\alpha, \kappa_\beta)$ must be zero on AB. The α-principal stress trajectories must, therefore, be straight lines. This considerably simplifies the analysis and the equilibrium equations can be integrated to give:

$$\left.\begin{aligned} M_\alpha &= M + A(\varphi) - \int q\rho_\beta \, d\rho_\beta + \frac{1}{\rho_\beta}\left(B(\varphi) + \int q\rho_\beta^2 \, d\rho_\beta\right) \\ M_\beta &= M \\ Q_\alpha &= \frac{A(\varphi)}{\rho_\beta} - \frac{1}{\rho_\beta}\int q\rho_\beta \, d\rho_\beta \\ Q_\beta &= 0 \end{aligned}\right\}. \tag{2.8}$$

The functions $A(\varphi)$ and $B(\varphi)$ are determined from the boundary conditions once the net of α- and β-lines has been determined. Massonnet [12] has solved a large number of problems of simply supported plates under point and distributed loads in each of which the plastic region lies entirely in this regime. The limiting factor in this regard is that the angle between a straight α-line and the normal to a simply supported edge cannot exceed 45° if the plastic state is in regime AB.

Regime B

Since $M_\alpha = -M$, $M_\beta = M$ equations (2.4) and (2.5) reduce to

$$Q_\alpha = -\frac{2M}{\rho_\beta}, \qquad Q_\beta = \frac{2M}{\rho_\alpha} \tag{2.9}$$

which when substituted into the remaining equilibrium equation (2.6) gives

$$-\frac{\partial}{\partial s_\alpha}\left(\frac{1}{\rho_\beta}\right) + \frac{\partial}{\partial s_\beta}\left(\frac{1}{\rho_\alpha}\right) - \frac{1}{\rho_\beta^2} + \frac{1}{\rho_\alpha^2} = -\frac{q}{2M}. \tag{2.10}$$

In the special case $q = 0$, (2.10) is the condition that the principal stress trajectories form a Hencky–Prandtl net [9, 10]. In this situation, therefore, we may expect to find an analogy between plate theory and the classical theory of slip-line fields. It is this point we wish to develop further here.

To make the analogy explicit, it is convenient to return to the equilibrium equations in the form (2.1)–(2.3). Since $q = 0$ the condition for vertical equilibrium (2.3) can be automatically satisfied if we introduce a stress function ψ for the shear forces defined by:

$$Q_x = -\frac{\partial \psi}{\partial y}, \qquad Q_y = \frac{\partial \psi}{\partial x}. \tag{2.11}$$

We have now only to consider the two moment equilibrium equations (2.1) and (2.2) which now become:

$$\frac{\partial M_x}{\partial x} + \frac{\partial}{\partial y}(M_{xy} + \psi) = 0 \tag{2.12}$$

and

$$\frac{\partial}{\partial x}(M_{xy}-\psi)+\frac{\partial M_y}{\partial y}=0 \tag{2.13}$$

from which we see that ψ can be thought of as an *isotropic or "hydrostatic" twisting moment.* The total "effective" moments acting on a typical elemental rectangle of the plate are hence as shown in Fig. 2(a). By introducing ψ we are simply replacing the shear forces by a statically equivalent set of twisting moments.

The stress function ψ is undefined with respect to an arbitrary additive constant, it can also be multivalued. The change in the value of ψ around a closed circuit Γ, traced in the anticlockwise sense, is equal to the total load applied to the region Σ bounded by Γ. (Since we have ruled out distributed loads, this will be due to point or line loads.) This is readily seen by considering the vertical equilibrium of Σ:

$$[\psi]=\oint_\Gamma \frac{\partial\psi}{\partial s}\,ds=\oint_\Gamma Q_n\,ds=\int_\Sigma q\,d\Sigma \tag{2.14}$$

(n being the inward normal to Γ).

An elemental curvilinear rectangular region whose sides are parallel to the principal stress trajectories is, when in regime B, subjected to the principal bending moments $\pm M$ and to the isotropic twisting moment ψ as shown in Fig. 2(b). The reader familiar with slip-line field theory will immediately identify this diagram with that for the equilibrium of a similar elemental region in plane strain (e.g. Fig. 12.3 of [2] or Fig. 21 of [7]) where now the α-, β-lines are the maximum shear stress trajectories (slip-lines) and the arrows represent

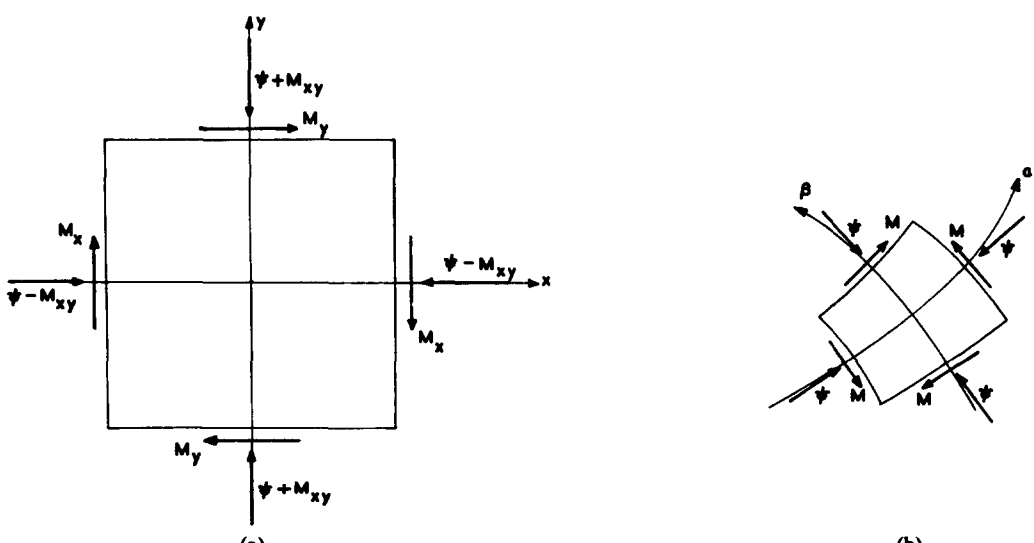

FIG. 2. Effective moment system acting on: (a) a typical rectangle in the (x, y) co-ordinate system; (b) a typical curvilinear rectangle whose sides are parallel to the α- and β-curves. (Moments act clockwise about direction of arrows.)

tractions instead of moments. The two stress states are identical under the transformation:

$$\varphi \leftrightarrow \varphi, \qquad M \leftrightarrow k, \qquad \psi \leftrightarrow p \tag{2.15}$$

k being the yield shear stress and p the hydrostatic pressure.

This isomorphism between the two stress states can alternatively be expressed in terms of Cartesian tensor components. Since the two principal bending moments are equal and opposite it follows, from the standard rules for the rotation of axes, that $M_x = -M_y$. Thus, referring to Fig. 2(a), we can interpret this plate stress state as a plane strain stress state using the transformation:

$$-M_x = M_y \leftrightarrow \tau_{xy}, \qquad M_{xy} \leftrightarrow \sigma'_x = -\sigma'_y, \qquad \psi \leftrightarrow p \tag{2.15a}$$

where $(\sigma'_x, \sigma'_y, \tau_{xy})$ are the Cartesian components of the two-dimensional stress deviator tensor. Under this correspondence equations (2.12) and (2.13) transform into the equilibrium equations for plane strain.

From the standard rules of rotation of axes the Cartesian components of the moment tensor for regime B are $(-M\cos 2\varphi, M\cos 2\varphi, -M\sin 2\varphi)$. Substituting in (2.13), (2.12):

$$\frac{\partial \psi}{\partial x} + 2M\cos 2\varphi \frac{\partial \varphi}{\partial x} + 2M\sin 2\varphi \frac{\partial \varphi}{\partial y} = 0 \tag{2.16}$$

$$\frac{\partial \psi}{\partial y} + 2M\sin 2\varphi \frac{\partial \varphi}{\partial x} - 2M\cos 2\varphi \frac{\partial \varphi}{\partial y} = 0 \tag{2.17}$$

which are identical with the corresponding equations for plane strain (cf. equation (21.1) in [8]). As is well known these equations are hyperbolic, with the α- and β-curves as characteristics and with invariant (Hencky) relations:

$$\left.\begin{aligned} \psi + 2M\varphi &= \text{const. on an } \alpha\text{-line} \\ \psi - 2M\varphi &= \text{const. on a } \beta\text{-line} \end{aligned}\right\}. \tag{2.18}$$

It follows that any statically admissible plane strain solution can be interpreted under the correspondence (2.15) as a statically admissible solution for a plate. Regions in the plane strain solution which are below yield will correspond to sub-yield regions in the plate solution whose stress state lies on the diagonal BD of the square yield locus [Fig. 1(a)]. This is because the symmetry of the stress tensor in plane strain implies that $-M_\alpha = M_\beta$ in the corresponding plate stress state. For the same reason it follows that plate stress states which are not on this diagonal have no analogue in plane strain.

There is a simple correspondence between the three commonest types of stress boundary condition:

TABLE 1

Plate boundary condition		Analogue in plane strain
(a) Simply supported (position fixed)	$\leftrightarrow$	Shear stress free
(b) Free edge	$\leftrightarrow$	Shear stress free with uniform normal traction
(c) Built in edge	$\leftrightarrow$	Perfectly rough

In (a) and (b) the α- and β-curves meet the boundary at 45° and in (c) either tangentially or at right angles. On a free edge the Kelvin–Tait condition must be satisfied, i.e.

$$Q_n - \frac{\partial M_{nt}}{\partial t} = 0 \tag{2.19}$$

which, using (2.11) and the fact that $M_{nt} = \pm M$, reduces simply to $\psi = \text{const.}$, corresponding to the uniform normal pressure condition in plane strain.

The theory of stress discontinuities in plane strain as described in [7, 8] can also be carried over *in toto* to plates. Across a stress discontinuity in a plate M_n and $Q_n - (\partial M_{nt}/\partial t)$ must be continuous. We can use (2.11) as above to write this second expression as $(\partial/\partial t)(\psi - M_{nt})$. The jump in $\psi - M_{nt}$ is hence constant along the length of the discontinuity; but since ψ is undefined with respect to an arbitrary additive constant, $\psi - M_{nt}$ can be made to be continuous across the discontinuity. Under the transformation (2.15a) M_n and $\psi - M_{nt}$ transform into τ_{nt} and σ_n respectively, which are precisely the quantities which have to be continuous across a stress jump in plane strain.

There is also a partial analogy between slip-line fields and the regime B for the square yield criterion but with different top and bottom reinforcement ($M_\alpha = -m$, $M_\beta = M$), and also regime B on the Tresca locus [Fig. 1(b); $M_\alpha = 0$, $M_\beta = M$]. The analysis is similar to the above except that $2M$ is replaced by $(M + m)$ or M in (2.16)–(2.18). The α-, β-curves still form a Hencky–Prandtl net, but now since the two principal bending moments are not equal and opposite, there is no *exact* correspondence between the stress states in the plate and in plane strain.

3. THE KINEMATIC ANALOGY—THE ANGULAR VELOCITY HODOGRAPH

The hodograph representation of deformation modes in plane strain was developed by Green [14] and Prager [15] (see also [16]). It has proved very useful as an aid to finding exact solutions, particularly by providing geometric formulations of kinematic boundary conditions. The basic properties of the corresponding "angular velocity hodograph" for plate deformation modes are derived in this section.

To begin with we will only assume that the material of the plate is isotropic, no particular yield criterion is specified. If v is the downward velocity of the plate, then the components of the angular velocity vector $\boldsymbol{\omega}$ referred to Cartesian axes are:

$$\omega_x = \frac{\partial v}{\partial y} \quad \text{and} \quad \omega_y = -\frac{\partial v}{\partial x}. \tag{3.1}$$

From the compatibility condition on v: $(\partial^2 v/\partial x \partial y) = (\partial^2 v/\partial y \partial x)$ it follows that:

$$\frac{\partial \omega_x}{\partial x} + \frac{\partial \omega_y}{\partial y} = 0. \tag{3.2}$$

If now we identify (ω_x, ω_y) as the components of a velocity vector in a plane strain deformation, (3.2) is the condition for the deformation to be isochoric, as it will be if the material is incompressible. It is this fact which lies at the root of Johnson's kinematic analogy.

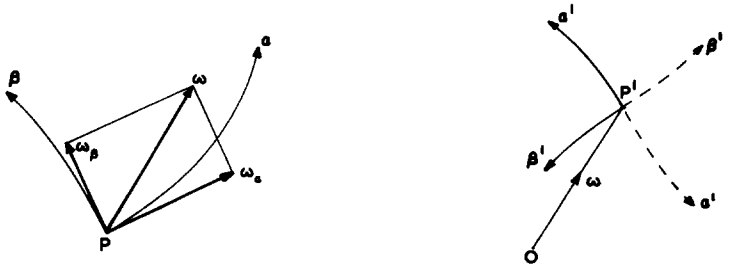

(a) (b)

FIG. 3. Angular velocity ω in: (a) physical plane; (b) velocity (or hodograph) plane.

As a result of the assumed isotropy the principal curvature trajectories coincide with the principal stress trajectories (α-, β-lines). The principal curvature rates are given in [11]:

$$\kappa_\alpha = -\frac{\partial^2 v}{\partial s_\alpha^2} - \frac{1}{\rho_\alpha}\frac{\partial v}{\partial s_\beta}, \qquad \kappa_\beta = -\frac{\partial^2 v}{\partial s_\beta^2} - \frac{1}{\rho_\beta}\frac{\partial v}{\partial s_\alpha}. \tag{3.3}$$

Since the rate of twist in the α- and β-directions are zero $\kappa_{\alpha\beta} = \kappa_{\beta\alpha} = 0$, so that

$$\frac{\partial^2 v}{\partial s_\alpha \partial s_\beta} - \frac{1}{\rho_\alpha}\frac{\partial v}{\partial s_\alpha} = \frac{\partial^2 v}{\partial s_\beta \partial s_\alpha} - \frac{1}{\rho_\beta}\frac{\partial v}{\partial s_\beta} = 0. \tag{3.4}$$

The components of the angular velocity vector $\boldsymbol{\omega}$ referred to the α-, β-system are [Fig. 3(a)]:

$$\omega_\alpha = \frac{\partial v}{\partial s_\beta} \quad \text{and} \quad \omega_\beta = -\frac{\partial v}{\partial s_\alpha} \tag{3.5}$$

so that

$$\kappa_\alpha = \frac{\partial \omega_\beta}{\partial s_\alpha} - \frac{\omega_\alpha}{\rho_\alpha} \quad \text{and} \quad \kappa_\beta = -\frac{\partial \omega_\alpha}{\partial s_\beta} + \frac{\omega_\beta}{\rho_\beta} \tag{3.6}$$

(3.4) can now be written:

$$\frac{\partial \omega_\alpha}{\partial s_\alpha} + \frac{\omega_\beta}{\rho_\alpha} = 0, \qquad \frac{\partial \omega_\beta}{\partial s_\beta} + \frac{\omega_\alpha}{\rho_\beta} = 0 \tag{3.7}$$

or equivalently

$$\left.\begin{aligned} \mathrm{d}\omega_\alpha - \omega_\beta \,\mathrm{d}\varphi = 0 \quad & \text{on an } \alpha\text{-line} \\ \mathrm{d}\omega_\beta + \omega_\alpha \,\mathrm{d}\varphi = 0 \quad & \text{on a } \beta\text{-line} \end{aligned}\right\}. \tag{3.8}$$

These equations are the exact analogues of Geiringer's equations in slip-line theory, under the correspondence

$$\varphi \leftrightarrow \varphi, \qquad \omega_\alpha \leftrightarrow u_\alpha, \qquad \omega_\beta \leftrightarrow u_\beta \tag{3.9}$$

where (u_α, u_β) are the components of velocity in the slip-line directions. However, it is to be emphasized that (3.8) *do not depend on whether or not the α-, β-curves form a Hencky–Prandtl net*, they are merely a statement that the *rates of twist* are zero in the principal

curvature directions. The corresponding statement in plane strain is that the rates of extension are zero in the maximum shear strain-rate directions (cf. [16]).

Just as in slip-line theory these equations can be given a simple interpretation in the velocity (or hodograph) plane. The angular velocity ω at a point P in the physical plane [Fig. 3(a)] is represented by a point P', with position vector $\boldsymbol{\omega}$ in the angular velocity hodograph [Fig. 3(b)]. As P traces out an α- (or β-) curve in the physical plane, P' traces out an image α'- (or β'-) curve in the hodograph plane. The geometric interpretation of (3.8) is that the α'- (or β'-) curve is *orthogonal* to the α- (or β-) curve at corresponding points (see for example [16] Sections 4, 5). If the α-, β-curves do happen to form a Hencky–Prandtl net it follows from this orthogonality property that the hodograph curves also form such a net.

If we denote the inclination of the α'-lines to the ω_x-axis in the ω-plane by $\varphi' = \varphi + \pi/2$ we can define the radii of curvature of the α'-, β'-curves by expressions analogous to (2.7):

$$\frac{1}{\rho_{\alpha'}} = -\frac{\partial \varphi'}{\partial s_{\alpha'}}, \qquad \frac{1}{\rho_{\beta'}} = \frac{\partial \varphi'}{\partial s_{\beta'}} \tag{3.10}$$

where $s_{\alpha'}$, $s_{\beta'}$ are the arc lengths of the α'-, β'-curves. The rates of change of the angular velocity component in the β-direction along an α-curve and vice-versa are given by:

$$\left.\begin{aligned} \frac{\mathrm{d}s_{\alpha'}}{\mathrm{d}s_{\alpha}} &= \frac{\partial \omega_\beta}{\partial s_\alpha} - \frac{\omega_\alpha}{\rho_\alpha} \\ \frac{\mathrm{d}s_{\beta'}}{\mathrm{d}s_{\beta}} &= -\frac{\partial \omega_\alpha}{\partial s_\beta} + \frac{\omega_\beta}{\rho_\beta} \end{aligned}\right\} \tag{3.11}$$

so that from (3.6) and (3.10)

$$\kappa_\alpha = \frac{\rho_{\alpha'}}{\rho_\alpha} = \frac{\mathrm{d}s_{\alpha'}}{\mathrm{d}s_\alpha} \quad \text{and} \quad \kappa_\beta = \frac{\rho_{\beta'}}{\rho_\beta} = \frac{\mathrm{d}s_{\beta'}}{\mathrm{d}s_\beta}. \tag{3.12}$$

We can use (3.12) to test whether, in any proposed solution, the "principal curvature-rate vector" $(\kappa_\alpha, \kappa_\beta)$ lies in the correct direction with reference to the current point on the yield locus. For example, at point B on the square Johansen locus [Fig. 1(a)] $\kappa_\alpha \leq 0$ and $\kappa_\beta \geq 0$ so that:

$$\frac{\rho_{\alpha'}}{\rho_\alpha} \leq 0 \quad \text{and} \quad \frac{\rho_{\beta'}}{\rho_\beta} \geq 0. \tag{3.13}$$

This condition is particularly simple since the *signs* of the four radii of curvature will be evident from the general form of the two nets. (3.13) is a stronger condition than the corresponding one in slip-line theory for a positive work-rate. As shown by Green [17] this is:

$$\frac{\rho_{\beta'}}{\rho_\beta} - \frac{\rho_{\alpha'}}{\rho_\alpha} \geq 0. \tag{3.14}$$

When interpreting a complete slip-line solution as a plate solution it is hence *always necessary to check that* (3.13) *is satisfied.*

Finally, it should be noted that, just as in slip-line theory where Geiringer's equations imply that a tangential velocity discontinuity across an α- or β-line is *constant* along its

length [7, 8, 16], equations (3.8) imply that a tangential discontinuity in angular velocity across a hinge line is constant along its length.

As an illustration of the use of the hodograph representation consider the conditions at a position fixed boundary. Since $v = 0$ on such a boundary the local angular velocity vector must be directed along the tangent to the edge. In particular if the edge is straight, the direction of the angular velocity vector will be constant along the edge, so that the image of the edge in the hodograph diagram is a parallel straight line. Johnson [1] makes frequent implicit use of this condition in the construction of upper-bound modes and a further example is given here in Fig. 5(d).

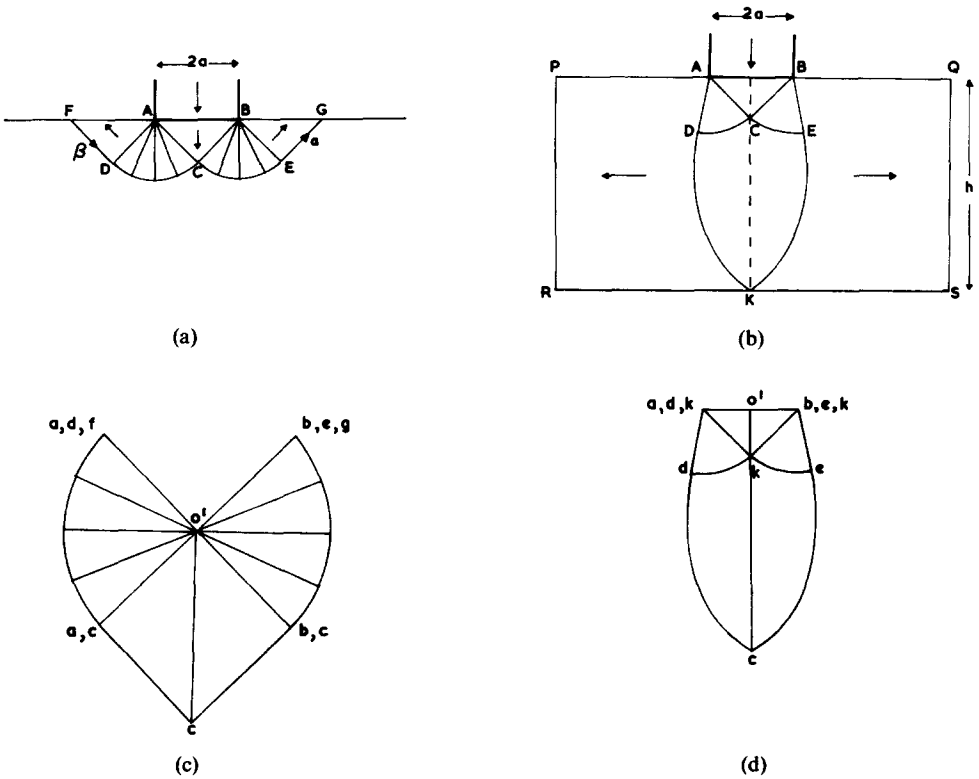

FIG. 4. Punch indentation: (a) Prandtl's solution for a half-space; (b) indentation of a plastic layer on a smooth foundation; (c) hodograph of (a); (d) hodograph of (b).

4. EXAMPLE—PLATE SUBJECT TO EDGE TWIST

As an example of a complete slip-line solution which can be interpreted as an exact plate solution, we consider the classic Prandtl solution for the indentation of a half-space by a rigid punch [Fig. 4(a)]. This is one of the examples considered in [1]. Following Johnson we interpret this solution as that for a plate subjected to a uniform twist along AB; all velocities in the plane strain solution being interpreted as angular velocities in the plate solution. The hodograph is shown in Fig. 4(c). We can show that this is in fact the exact solution using the analogy developed in Section 2.

The plastic region is everywhere in regime B, so that $M_\alpha = -M$, $M_\beta = M$. In the constant state regions ADF and BEG the twisting moment is $-M$ on the free boundaries AF and BG. Without loss of generality we can take $\psi = 0$ in these two regions, so that from (2.18) $\psi = \pi M$ in ABC. The twisting moment on AB is M, so that the total "effective" twisting moment on the boundary jumps by $(2+\pi)M$ at A and B indicating that equal and opposite point loads of magnitude $(2+\pi)M$ act at these two points. The total applied torque is hence $2(2+\pi)Ma$ which corresponds to the total punch load.

The Prandtl solution has been shown to be complete by Bishop [18] who constructed a statically admissible stress field in the rigid region (see also Salençon [19]. The arguments of Section 2 show that the analogous plate solution is hence also complete. The value of the applied torque given above agrees, of course, with that deduced by Johnson from work-rate considerations. The present arguments, however, show that this solution *is exact and not merely an upper bound.*

The plane strain solution for the punch indentation of a plastic layer resting on a smooth foundation [Fig. 4(b)] can similarly be interpreted as a plate solution. If $(h/a) > 8{\cdot}7$ (approx) the solution is still Prandtl's, but for smaller values of (h/a) the deformation spreads to the foundation as shown in Fig. 4(b) (cf. [7]). In the analogous plate problem the foundation RKS is interpreted as a position fixed boundary; whilst the rigid regions $APRK$ and $BQSK$, which in the plane strain solution move apart with equal speeds, rotate about RKS with equal speeds but opposite senses. Once the pressure is known at one point of the plastic zone—K say, it can be deduced at every other point from Hencky's relations. The pressure at K is determined from the condition that there is no net horizontal force on ADK or BEK. The corresponding condition in the plate problem, which determines ψ throughout the plastic zone, is that there should be no net horizontal couple on ADK or BEK. The two stress fields are hence completely analogous and the yield point load on the punch can be interpreted as the yield point torque on the plate (cf. [1]).

5. EXAMPLE—POSITION FIXED RECTANGULAR PLATE WITH CENTRAL POINT LOAD

The upper bound solutions of yield-line theory for this problem are shown in Figs. 5(a) and (b). The corresponding limit loads P are plotted in Fig. 6 as a function of aspect ratio. Massonnet [12] has shown that the solution in Fig. 5(a) is the exact solution for a *square* plate. He employs a radial associated stress field, the plastic stress state lying entirely in regime AB. An alternative associated stress field which lies entirely in regime B is shown in Fig. 7. It consists of four regions in each of which the stress state is one of homogeneous "biaxial twist" separated by straight stress discontinuities OP, OQ, OR and OS. Equilibrium is ensured across each of these discontinuities since the *normal* components of the twist and bending moments are continuous. These biaxial twist states are the analogues of the biaxial tension (or compression) states in plane strain. (Such states are frequently used to construct lower bound solutions to boundary value problems in plane strain, cf. Drucker and Chen [20].) Each of these four stress states is at yield, since the difference between the two twist components is $2M$. The isotropic twist ψ, arising from the shear force distribution, is the average of the two twist components [cf. Fig. 2(a)]. The value of ψ hence jumps by $2M$ across each stress discontinuity, and increases by $8M$ in one complete (anticlockwise) circuit around 0. The associated yield point load is hence

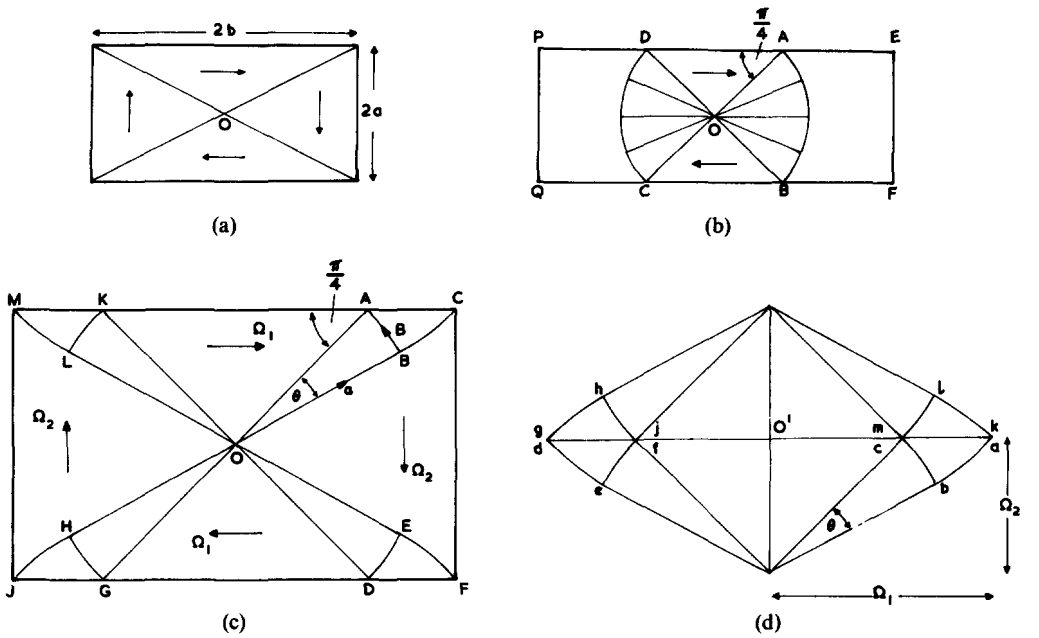

FIG. 5. Simply supported rectangular plate centrally loaded by a point load: (a), (b) yield-line theory upper bound solutions; (c) improved upper bound solution for $1 < b/a < 2{\cdot}21$; (d) hodograph of (c).

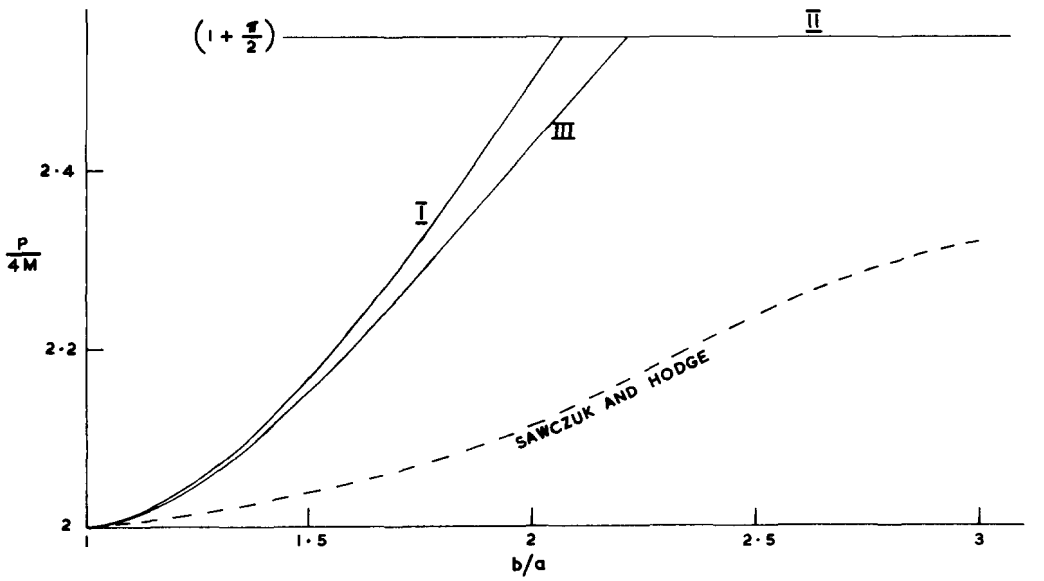

FIG. 6. Variation of upper bounds to $P/4M$ with aspect ratio: *I*-solution (a); *II*-solution (b); *III*-solution (c). Solution *II* is exact for $b/a \geq 3{\cdot}10$, cf. Section 6.

$8M$ from (2.14), which coincides with the value obtained from the upper bound calculation and is, therefore, exact.

This same type of stress field provides a lower bound ($P = 8M$) for a *rectangular* plate, but this does not now coincide with the upper bound value. Moreover, since now the angle between a radius vector from 0 and the normal to the plate boundary will, in places, be greater than 45° we cannot expect to find a complete solution whose stress state lies entirely in regime AB [10, 12].

A rather better upper bound mode can be found for $1 < b/a < 2{\cdot}21$ from the solution shown in Figs. 5(c) and (d). Regions OAK, OCF, ODG and OJM rotate rigidly about the boundaries, hingelines form along OBC, OLM, OHJ and OEF, whilst the deformation is continuous in the remaining regions. OAB is a centred fan, whilst ABC is the Hencky–Prandtl net defined by the circular arc AB and its reflection in AC. All the α- and β-curves will hence intersect AC at 45°. The angle θ is hence determined uniquely by the aspect ratio b/a.

Suppose now we specify the value of ψ on OA, its value on OK is then determined by the condition that OAK should be in overall equilibrium, in particular the resultant moment in the direction parallel to AK must be zero. The values of ψ along OLM are then obtained from (2.18). We can then use the condition that $MLOHJ$ must be in equilibrium to calculate ψ along OHJ. In this way we can calculate ψ in all the deforming regions, and the change in ψ in one complete circuit around 0 gives the value of P.

An alternative method of calculating P which is quicker in practice, but which does not give the same insight into the problem, is to perform a work calculation. The rate of energy dissipation in the Hencky–Prandtl nets can be lifted from the calculations already performed for plane strain problems in which these particular nets occur (e.g. the punch indentation problem considered in the last section). The resulting loads are plotted in Fig. 6.

In order to show that this was the exact solution, it would be necessary to demonstrate the existence of statically admissible stress fields in the four rigid regions. This is easy to do in OAK and OGD, either by using Massonnet's radial stress fields or the biaxial twist states used in Fig. 7. However, no such solutions have yet been found for the two remaining regions, so that this solution must be regarded, at present, as only an upper bound solution.

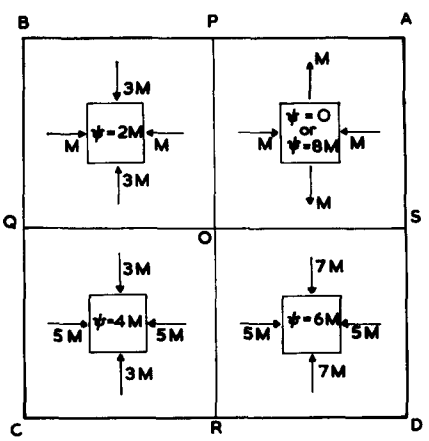

FIG. 7. Statically admissible solution for centrally loaded, simply supported, square plate.

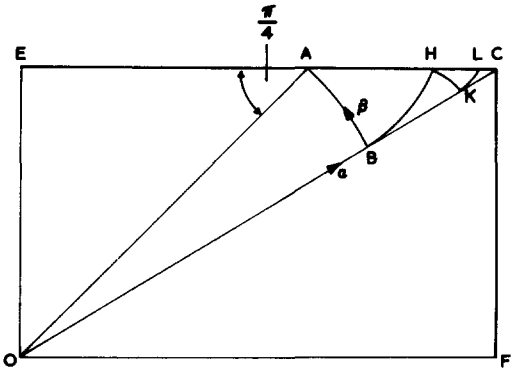

FIG. 8. Quadrant of solution for centrally loaded, simply supported, rectangular plate given in [10].

Sawczuk and Hodge [10] have proposed a rather similar solution, a quadrant of which is shown in Fig. 8. The stress states in OAE and OCF are in regime AB, the α-lines being radial straight lines and the β-lines circular arcs. The stress state in $OACB$ is in regime B, OAB is a centred fan, whilst the net in ACB is constructed from AB using the fact that the α-lines must meet the plate boundary AC at 45° and the line BC tangentially. BC is an envelope of α-lines—a so called "limiting line" [8]. Sawczuk and Hodge present this solution as statically admissible, with loads which as shown in Fig. 6 are appreciably lower than those given by the yield-line theory solutions. However, there is an error in their analysis and indeed it is shown in the next section that the yield-line solution of Fig. 5(b) is, in fact, the *exact* solution for aspect ratios greater than $\sqrt{(2)}e^{\pi/4}$.

The error in the solution in Fig. 8 is that there is an inadmissible discontinuity in the shear forces across BC. For equilibrium the shear force component Q_β must be continuous across BC (cf. [11]). In $OBCF$ the stress system is in regime AB so that $Q_\beta = 0$ (2·8). ABC is in regime B so that $Q_\beta = 2M/\rho_\alpha$ (2.9). Thus, Q_β will only be continuous if ρ_α is infinite on BC. However, in general, this condition will not be met; the only condition necessarily satisfied on an envelope of α-lines is that $\rho_\beta = 0$ (see, for example [7] or [8]).† The same remarks apply to the solution for an elliptic plate given in [10] and the generalization to orthotropic plates given in [21].

An alternative way of viewing this is to note that a possible deformation mode associated with this solution is the simple collapse mechanism shown in Fig. 5(a). However, the work calculation for this mode, does not give the same yield-point load as the stress solution (see Fig. 6), again indicating that this latter field cannot possibly be statically admissible.

6. COMPLETION OF YIELD-LINE SOLUTION FOR $b/a \geq \sqrt{(2)}e^{\pi/4}$

The solution of Fig. 5(b) will be exact if we can show that statically admissible stress fields exist in the proposed rigid regions. This is readily done in the triangular regions OAD, OBC using either a Massonnet-type radial field or two "biaxial twist" states separated by a stress discontinuity (cf. Fig. 7). The real problem is to continue the stress field into the regions $AEFB$ and $DPQC$. We do this here using the technique developed

† This situation is not rectified if instead of insisting on Q_β being continuous we use the weaker Kelvin–Tait condition, since the normal component of the twisting moment is zero on both sides of BC.

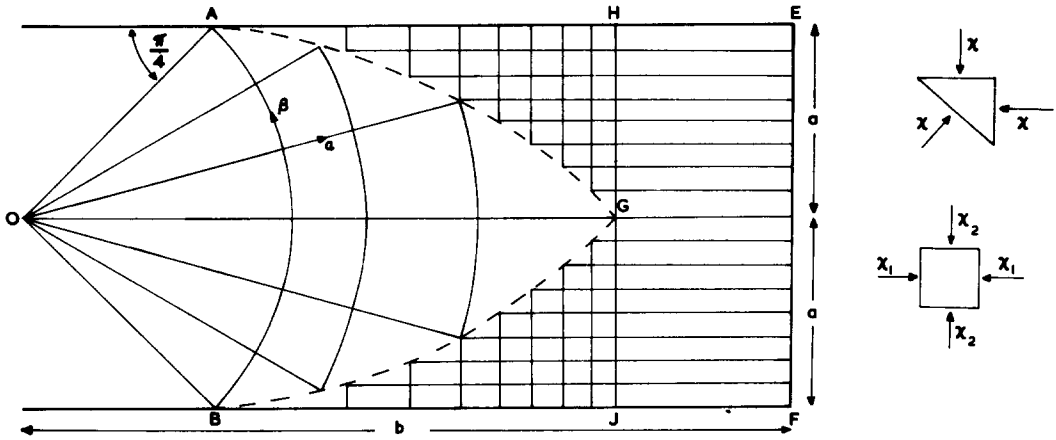

FIG. 9. Completion of the yield-line theory solution of Fig. 5(b) when $b/a \geq \sqrt{(2)}\,e^{\pi/4}$.

by Bishop [18] for plane strain solutions. The particular construction used is very similar to that employed by Alexander [22] to complete a number of extrusion solutions.

One half of the solution is shown in Fig. 9. The centred fan OAB is continued into $AEFB$, but is bounded by the curves AG and BG. These are the trajectories, starting from A and B, which bisect the α- and β-curves. In plane strain they would be principal stress trajectories but in the plate are the trajectories of maximum twisting moment. For this particular net these trajectories are logarithmic spirals and OG is of length $a\sqrt{(2)}\,e^{\pi/4}$. We can now construct an equilibrium stress field in the rest of the plate, which both satisfies the boundary conditions and does not violate the yield criterion as follows.

The region $AEFB$ is divided up into an infinite number of *elemental* rectangles and triangles by two mutually orthogonal families of parallel straight lines as illustrated schematically in Fig. 9. Since AG and BG are maximum twisting moment trajectories the curvilinear faces of the elemental triangles bordering on these curves are not subject to any bending moment, only to an "effective" twisting moment—χ say. The variation of the stress-function ψ on AG or BG can be deduced from (2.18), for since the α-lines are straight in ABG, ψ is constant along each of them. So from the second of (2.18), $\psi = 2M\varphi$ on AG and BG, where φ is the anticlockwise inclination of the local α-line to OG and the arbitrary constant in the definition of the stress function has been chosen so that $\psi = 0$ on OG. Combining this ψ with the actual twisting moment gives the total "effective" twisting moment as $\chi = (2\varphi - 1)M$ on AG and $(2\varphi + 1)M$ on BG.

Each of the elemental triangular regions bordering on AG and BG will be in equilibrium if the two orthogonal faces are also subject to the same "effective" twisting moment χ (Fig. 9, insert). The resulting stress state is therefore purely isotropic.

The *longitudinal* component of the *effective* twisting moment is now taken to be constant in each of the horizontal and vertical strips, so that each *elemental* rectangular region in AHG and BJG is subjected to a *biaxial twist* (Fig. 9, lower insert). This stress-state is hence in equilibrium by construction and satisfies the zero normal bending moment condition on the plate boundaries. It will also be statically admissible if the magnitude of the principal bending moments $(= \frac{1}{2}|\chi_1 - \chi_2|)$ nowhere exceeds the yield moment M.

The greatest difference between χ_1 and χ_2 occurs at H and J where $\frac{1}{2}|\chi_1 - \chi_2| = (\pi M/4) < M$ so that this stress field is indeed statically admissible.

Finally, we can continue this field into $HEFJ$ by taking χ_1 as defined above and putting $\chi_2 = 0$ everywhere. The magnitude of the principal bending moment never exceeds $\frac{1}{2}M$ in this region, so this stress field is also statically admissible.

The solution has hence been shown to be complete whenever $b \geq a\sqrt{(2)}\,e^{\pi/4}$.

7. DISCUSSION

One of the main difficulties in constructing solutions to plane strain boundary value problems in rigid/plasticity theory is that there is no way of knowing, *a priori*, whether any given part of the body is deforming plastically or remaining rigid. The technique of solution must therefore inevitably involve some element of trial and error. There is an extra complication in plate theory in that there are two (or more, depending on the yield criterion) possible types of plastic regime, e.g. edge and corner regimes for a piece-wise linear yield locus. Again there would seem to be no method of knowing, in advance, the position of the boundaries between these various regimes.

For the square yield locus Massonnet [12] has established a large class of solutions in all of which the entire plate is in an edge-regime [regime AB in Fig. 1(a)]. The analogy established here shows that there is another class of solutions, in which the plastic state is everywhere in a corner-regime [regime B in Fig. 1(a)]. Each of these solutions has an analogue in plane-strain. In nearly all the solved plane strain problems of practical interest in metal forming processes the load is applied by a uniformly moving rigid toolpiece. This corresponds in plate theory to a torque applied through a uniform twist on the plate edge. Such loading conditions are of very little practical interest, so that the interpretation of known plane strain solutions has not been pursued beyond the two examples discussed in Section 4. The examples discussed in Sections 5 and 6 however illustrate that some of the standard techniques of slip-line field theory, such as the hodograph diagram and Bishop's method of completing solutions, may prove very useful in constructing new plate solutions.

Acknowledgements—I am very grateful to Professor H. G. Hopkins and Professor W. Johnson for some helpful comments on this work.

REFERENCES

[1] W. JOHNSON, *Int. J. mech. Sci.* **11**, 913 (1969).
[2] W. JOHNSON and P. B. MELLOR, *Plasticity for Mechanical Engineers*. Van Nostrand (1962).
[3] K. W. JOHANSEN, *Brudlinieteorier*. Copenhagen (1943); English edition: *Yield-line Theory*. Cement and Concrete Association (1962).
[4] R. H. WOOD, *Plastic and Elastic Design of Slabs and Plates*. Thames and Hudson (1961).
[5] L. L. JONES and R. H. WOOD, *Yield Line Analysis of Slabs*. Thames and Hudson (1967).
[6] A. SAWCZUK and T. JAEGER, *Grenztragfähigkeits-Theorie der Platten*. Springer-Verlag (1963).
[7] R. HILL, *The Mathematical Theory of Plasticity*. Clarendon Press (1950).
[8] W. PRAGER and P. G. HODGE, *The Theory of Perfectly Plastic Solids*. Wiley (1951).
[9] W. SCHUMANN, *Q. appl. Math.* **16**, 61 (1958).
[10] A. SAWCZUK and P. G. HODGE, *J. appl. Mech.* **35**, 357 (1968).
[11] H. G. HOPKINS, *Proc. R. Soc.* **A241**, 153 (1957).
[12] CH. MASSONNET, *Mag. Concr. Res.* **19**, 13 (1967).

[13] P. G. HODGE, *Q. appl. Math.* **22**, 74 (1964).
[14] A. P. GREEN, *J. Mech. Phys. Solids* **2**, 73 (1954).
[15] W. PRAGER, *K. tek. Högsk. Handl.* No. 65 (1953).
[16] W. PRAGER, *Introduction to Plasticity*. Addison-Wesley (1959).
[17] A. P. GREEN, *Q. Jl Mech. appl. Math.* **6**, 223 (1953).
[18] J. F. W. BISHOP, *J. Mech. Phys. Solids* **2**, 43 (1953).
[19] J. SALENCON, *C.r. hebd. Séanc. Acad. Sci., Paris* **A264**, 613 (1967).
[20] D. C. DRUCKER and W. F. CHEN, *Engineering Plasticity*, edited by J. HEYMAN and F. A. LECKIE, p. 129 (1968).
[21] A. SAWCZUK, *Int. J. Solids Struct.* **5**, 227 (1969).
[22] J. M. ALEXANDER, *Q. appl. Math.* **19**, 31 (1961).

(*Received* 15 *May* 1970; *revised* 26 *September* 1970)

Абстракт—Работа представляет теорию, покрощейся на основании современной аналогии Джонсона между рещениями, касающимися верхних пределов, для жестких или идеально пластических материалов, в области плоской деформации и теории изгиба пластинок. Эта аналогия обобщается на полные решения для нижнего предела. Можно выяснить много строгих решений задач плоской деформадии, таких как классическое решение штампа Прандтля, при помощи точных решений задач изгиба пластинок. В качестве иллюстрации способа поля линий скольжения, который можно включть в теорию пластинок, используется метод Бишопа полных решений линий скольжения, с целью заключения полностью решений теории пчлстических тирнчров для дентрически нагруженной, свободно опертой, прямоугольной пластинки. Оказывается, что недавные решения этих и подобных задач, полученные Савчуком и Ходжем, ошибочные.